Ligand-field atomic-multiplet calculations for arbitrary symmetry

Alessandro Mirone and Maurizio Sacchi
Laboratoire pour l'Utilisation du Rayonnement Electromagnétique, Centre Universitaire Paris-Sud, Boîte Postal 34, 91898 Orsay, France

Susana Gota
SRSIM-DRECAM, CEA Saclay Bâtiment 462, Centre d'Etudes Nucleaires, 91191 Gif-sur-Yvette, France
(Received 15 November 1999)

We have developed a calculational method for ligand-field multiplets. In our method the effect of the perturbations surrounding the considered atom is described by a monoelectronic potential interacting with the external electrons and the Hamiltonian is obtained by summing all the intra-atomic interactions and the external perturbations at once. Our method does not require any assumptions regarding the hierarchy of interaction terms and can treat any geometry, even in the absence of any nontrivial symmetry group. We have applied this method to the case of nickel $2p$ edges in Ni-phthalocyanine and to study the experimental absorption spectra and magnetic circular dichroic reflectivity of a thin Fe_3O_4 film.

I. INTRODUCTION

The ligand-field atomic-multiplet theory is a very successful approach to the description of atomic transitions in localized electronic systems and solids.[1] This theory is able to calculate with good experimental agreement the multiplet structure of core-to-$3d$ excitations in transition metals and core-to-$4f$ excitations in rare earths. The multiplet structure is very sensitive to the atomic environment and strongly depends on the electronic structure of the atom undergoing the transition. The availability of tunable high-resolution x-ray sources allows one to resolve these structures and, in this way, to study the atomic environment by fitting the calculated spectra to the experiment.[2] Moreover, the strong Z dependence of core level energies makes this technique element selective and one can study separately the contributions from different elements entering a given compound.

The ligand-field atomic model was first developed by Yamaguchi *et al.*[3] and was more completely generalized in the works of Thole, van der Laan, and co-workers.[4–6] Their method is based on the choice of a given coupling, the calculation of the atomic states, and their projection on the basis of irreducible representations of the ligand-field symmetry group. So far their calculation procedure has been worked out for a limited set of crystal geometries, and in principle can be applied to any geometry by use of the Butler's point group program.[7]

The procedure that we present in this paper[8] is based on the same essential physical assumptions as that of Thole and co-workers but does not use group theory and does not require any assumptions regarding the hierarchy of interaction terms. For this reason it is immediately applicable to any geometry regardless of the ligand-field symmetry group. We discuss the theoretical basis of our method in the next section, in Sec. III we describe the numerical procedure, while in Sec. IV some numerical results are discussed in comparison with experiments.

II. THEORETICAL BASIS

We consider the Hamiltonian of an isolated atom consisting of intra-atomic interactions plus perturbation terms describing the effect of the neighboring atoms. The contribution of electrostatic interactions involving one or two electrons in external orbitals is reduced in order to simulate multiconfiguration and hybridization effects.[9] This consists in multiplying the core-valence and valence-valence Slater integrals by a factor that is taken as a free parameter. For magnetic materials the local exchange field is described by an interaction term that is proportional to the projection S_z of the spin along the magnetization axis.

The effect of the perturbing neighboring atoms and their geometry is described by a monoelectronic potential acting on the valence electrons. For an atom having an open external shell with angular moment l we describe this monoelectronic potential as a $(2\times l+1)\times(2\times l+1)$ matrix C, which gives the matrix elements of the potential between the monoelectronic levels of the shell. In the basis that diagonalizes the angular momentum, this matrix is constructed as follows. For just one perturbing atom lying along the angular moment quantization axis z we write C as C_z:

$$C_{z,(m_{za},m_{zb})}=\begin{cases}\delta & \text{for } m_{za}=m_{zb}=0\\ 0 & \text{otherwise,}\end{cases} \tag{1}$$

where δ is a free parameter. The only nonzero element in Eq. (1) is the one acting on the $m_z=0$ levels. We assume that all the other elements are zeroed by the centrifugal force that pushes the electron away from the z axis. This is the simplest assumption. One could eventually assume a more complex form for C_z allowing other diagonal elements to be nonzero. To study the effect of the rotational symmetry breaking induced by a nonspherical perturbing atom located along the z axis, nonzero off-diagonal terms should be considered. In the examples reported in this paper we have always used the simple form of Eq. (1) which requires just one free parameter.

In a more general case, n identical neighbors lie at the same distance around the absorbing atom. The matrix C is then constructed by similitude transforming the matrix of Eq. (1) for each neighbor to a system where it lies on the z axis, and by summing over all n positions:

$$C=\sum_j D_j C_z D_j^{-1}, \tag{2}$$

where C_z is the matrix of Eq. (1) and D_j is the rotation matrix that brings the jth atom onto the z axis. Equation (2) can easily be generalized to the case where not all the neighbors lie at the same distance. In this case, in order to avoid a proliferation of free parameters, it is useful to introduce a scaling law with distance for the parameter δ in Eq. (1).

III. NUMERICAL PROCEDURE

Our code first calculates the orbitals $\psi_{n,l}$ self-consistently with a spherical local-density approximation (LDA) monoelectronic potential. This potential depends on the local charge density $\rho(x)$ given by a sum over the electron orbitals:

$$\rho(r)=\sum_{j=1}^{N_{\rm el}} |\psi_{n_j,l_j}(r)|^2=\sum_{n,l} |\psi_{n,l}(r)|^2 f_{n,l}, \tag{3}$$

$N_{\rm el}$ being the number of electrons and $f_{n,l}$ the occupation number of the (n,l) shell. The potential is written (in atomic units) as[10]

$$V(r)=\mathrm{Min}\left(-\frac{Z}{r}+V_\rho(r)-\frac{0.916\,33}{1.5 r_s(r)};-\frac{Z-N_{\rm el}+1}{r}\right), \tag{4}$$

where $V_\rho(r)$ is the solution to the Poisson equation for the charge density $\rho(r)$, Z is the nuclear charge, and r_s is

$$r_s^{-1}(r)=\left(\frac{4\pi\rho(r)}{3}\right)^{1/3}. \tag{5}$$

The orbitals $\psi_{n,l}$ are given by the solutions of the nonrelativistic Schrödinger equation in the potential $V(r)$.

Once a self-consistent set of $\psi_{n,l}$ is found, we calculate all the intra-atomic interactions. This means Slater integrals (with reduction for hybridization), the kinetic part (the Laplacian of the $\psi_{n,l}$ functions), and the spin-orbit interaction. The spin-orbit matrix element between two monoelectronic levels a and b is calculated as

$$\left\langle n_b,l_b,m_b,s_b\left|\alpha^2\frac{|E_{n_a,l_a}(r)|}{2r}SL\right|n_a,l_a,m_a,s_a\right\rangle, \tag{6}$$

where $E_{n_a,l_a}(r)$ is the electric field given by the nuclear charge and by a reduced electronic charge density $\rho_{n_a,l_a}(r)$ obtained by removing one electron from the (n_a,l_a) shell in Eq. (3):

$$\rho(r)_{n_a,l_a}=\sum_{n,l} |\psi_{n,l}(r)|^2[f_{n,l}-\delta(n,n_a)\delta(l,l_a)]. \tag{7}$$

The intra-atomic interaction and the perturbation potential of Eq. (2) are then used to compose the Hamiltonian matrix.

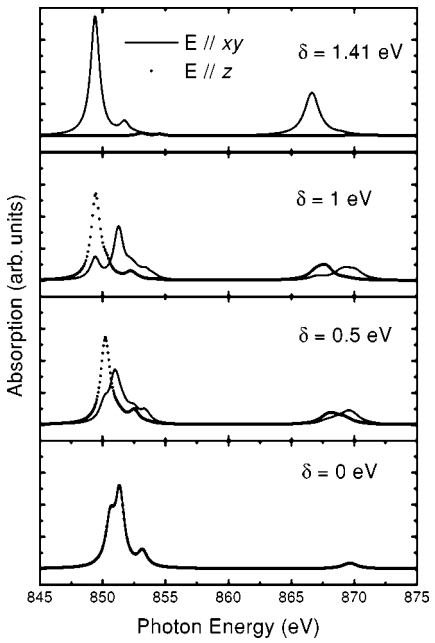

FIG. 1. Calculated $2p\rightarrow 3d$ absorption spectra for Ni $3d^8$ in Ni-phthalocyanine. Curves for E parallel (lines) and perpendicular (dots) to the xy nitrogen plane are reported for four different values of the parameter δ. The calculations have been done applying a 75% reduction of $3d$-$3d$ and $3d$-$2p$ Slater integrals.

The Hamiltonian operates on a Fock space that is spanned by a basis of determinants. Both the basis and the Hamiltonian are constructed automatically by the program. The diagonalization of the Hamiltonian gives the atomic multiplet states and their energy.

In the next section we show examples of calculated absorption spectra. These spectra are calculated in the dipolar approximation. These calculations involve the diagonalization of two Hamiltonians, one for the base configuration and the other for the excited one, and finally the calculation of dipolar elements between the atomic states of the two configurations. Finite-temperature effects are taken into account by a Boltzmann average over the states of the base configuration.

IV. APPLICATIONS AND COMPARISON TO EXPERIMENTS

We discuss in this section the $2p\rightarrow 3d$ transitions in the case of a nickel phthalocyanine molecule (NiPc) and of a ferrimagnetic Fe_3O_4 thin layer. In the NiPc molecule, Ni is surrounded by four nitrogen atoms in planar configuration. The perturbation matrix C of Eq. (2) for the nickel $3d$ shell, assuming the simplest form of C_z given by Eq. (1) and taking the quantization axis z perpendicular to the xy nitrogen plane, is

$$C=4\times\delta\times\begin{pmatrix} \frac{3}{8} & 0 & 0 & 0 & \frac{3}{8} \\ 0 & 0 & 0 & 0 & 0 \\ 0 & 0 & \frac{1}{4} & 0 & 0 \\ 0 & 0 & 0 & 0 & 0 \\ \frac{3}{8} & 0 & 0 & 0 & \frac{3}{8} \end{pmatrix}. \tag{8}$$

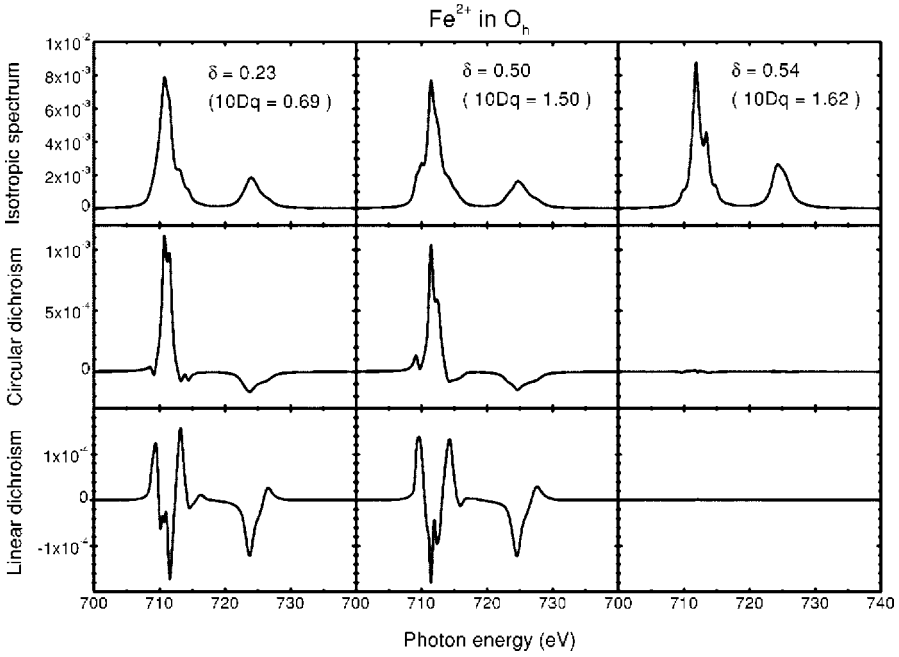

FIG. 2. Calculated absorption and dichroism (circular and linear) for Fe^{2+} in octahedral sites. The calculations are done with an 80% reduction of $2p$-$3d$ and $3d$-$3d$ Slater integrals, with a local exchange field oriented along the [100] axis, and considering three values of δ. Between $\delta=0.50$ and 0.54 eV the system undergoes a high-spin to low-spin transition. Absorption spectra are expressed as the imaginary part of the optical index.

Figure 1 shows the calculated nickel $2p\rightarrow 3d$ absorption spectra for linearly polarized x rays: curves for E parallel (lines) and perpendicular (dots) to the xy nitrogen plane are reported, for four different values of the parameter δ. Values of δ range from 0 eV at the bottom of the figure to 1.4 eV at the top. The calculations have been done assuming a nickel $3d^8$ electronic configuration and applying a 75% reduction to $3d$-$3d$ and $3d$-$2p$ Slater integrals. At $\delta=0$ the system is spherically symmetric and the two orientations of the polarization vector E give equivalent results. As soon as the perturbation is switched on, the absorption becomes polarization dependent. When δ increases from 1 to 1.41 eV, the system undergoes a high-spin to low-spin transition, related to the nitrogen atoms pushing the nickel $3d$ electrons away from the plane. When the perturbation is strong enough, the two holes of Ni $3d^8$ are both in the xy plane, on the same $d_{x^2-y^2}$ orbital. In this case the absorption is zero when E is along the z axis, since the transitions from a $2p$ ($2p_x$, $2p_y$, or $2p_z$) level to a $3d_{x^2-y^2}$ hole are forbidden for the z component of the dipolar interaction. The multiplet structure and the polarization dependence shown in Fig. 1 at $\delta=1.41$ eV fit well the experimental observations reported in the literature for this compound.[11]

The ferrimagnetic Fe_3O_4 system presents three distinct Fe sites, of octahedral and tetrahedral symmetry. The tetrahedral site is occupied by Fe^{3+} ions while half of the octahedral sites are occupied by Fe^{3+} and the other half by Fe^{2+} ions. The octahedral sites are surrounded by six neighbors whose contributions to C of Eq. (2) sum up to

$$C_{O_h}=6\times\delta_{O_h}\times\begin{pmatrix}\frac{1}{4}&0&0&0&\frac{1}{4}\\0&0&0&0&0\\0&0&\frac{1}{2}&0&0\\0&0&0&0&0\\\frac{1}{4}&0&0&0&\frac{1}{4}\end{pmatrix}, \tag{9}$$

while for the tetrahedral sites

$$C_{T_d}=4\times\delta_{T_d}\times\begin{pmatrix}\frac{1}{6}&0&0&0&\frac{-1}{6}\\0&\frac{1}{3}&0&0&0\\0&0&0&0&0\\0&0&0&\frac{1}{3}&0\\\frac{-1}{6}&0&0&0&\frac{1}{6}\end{pmatrix}. \tag{10}$$

The perturbation splits the degenerate $3d$ orbitals into two energy levels separated by $3\,\delta_{O_h}$ and $\frac{4}{3}\,\delta_{T_d}$ for octahedral and tetrahedral symmetry, respectively. In the literature this splitting is expressed by the symbol $10Dq$.[1]

The absorption at the Fe $2p\rightarrow 3d$ resonance is the sum of the contributions from the octahedral Fe^{2+} site, the tetrahedral Fe^{3+} site, and the octahedral Fe^{3+} site. Each calculated contribution is a function of the Slater integral reduction factors, of the perturbing field strength δ, and of the local exchange field. Figure 2, for example, illustrates the dependence on δ_{O_h} of the contribution from the octahedral Fe^{2+} site. The calculations are done with an 80% reduction of $2p$-$3d$ and $3d$-$3d$ Slater integrals, with a local exchange field oriented along the [100] axis, and considering three values of δ_{O_h}. The Boltzmann average is performed at room temperature. The isotropic spectrum is given by $I_1+I_0+I_{-1}$, where I_0 is the absorption for light linearly polarized parallel to the quantization axis and $I_{\pm 1}$ refer to circular polarization parallel or antiparallel to the quantization axis. The linear and circular dichroism spectra are given by $I_1-2I_0+I_{-1}$ and I_1-I_{-1}, respectively. The absorption and dichroism are sensitive to variation of δ_{O_h}. At $\delta_{O_h}=0.23$ eV and at $\delta_{O_h}=0.50$ eV, the octahedral Fe^{2+} site displays both linear and circular dichroism, the former being one order of magnitude smaller than the latter. Between $\delta_{O_h}=0.50$ eV and $\delta_{O_h}=0.54$ eV the system undergoes a high-spin to low-spin transition and dichroism becomes vanishingly small.

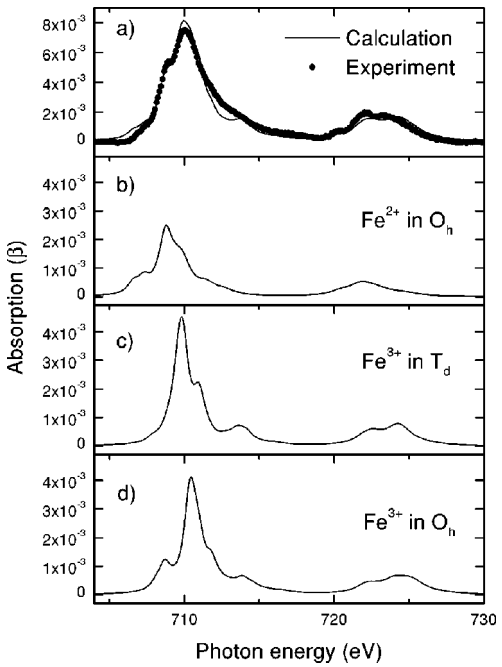

FIG. 3. $2p \rightarrow 3d$ absorption spectra of Fe_3O_4. (a) Comparison between the result of our model calculation and the experimental curve; (b)–(d) site-resolved contributions to the total absorption spectrum of Fe_3O_4.

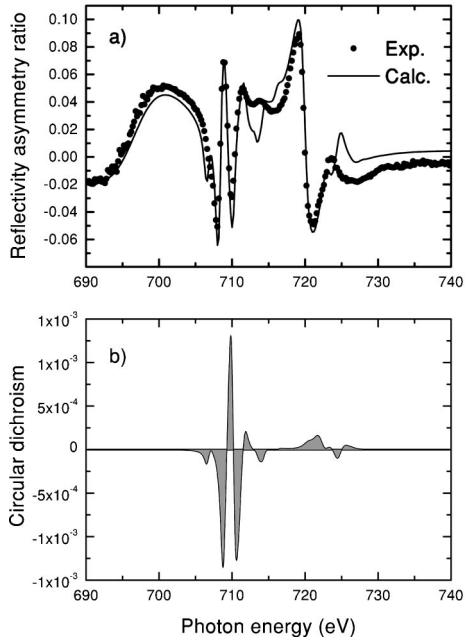

FIG. 4. (a) Experimental and calculated magnetic asymmetry ratio in the resonant reflectivity of circularly polarized photons (see text); (b) calculated magnetic circular dichroism at the $2p$ absorption edge.

We will now discuss the comparison between our calculations and experimental results for the Fe_3O_4 thin film, with reference to recent work by Kuiper *et al.*[2] on Fe $2p$ absorption and dichroism in this same compound. The experimental absorption in Fig. 3(a) refers to an 80-Å-thick $Fe_3O_4(111)$ film epitaxially grown on alumina.[13] Data were collected at room temperature with the linear polarization vector of the light along the $[0\bar{1}1]$ direction and the magnetic polarization along the $[\bar{2}11]$ axis. Previous work[12] has suggested that the arrangement of Fe^{3+} and Fe^{2+} octahedral sites in the Fe_3O_4 crystal may vary from an ordered charge configuration to disordered across the Verwey insulator/metal transition at about 121 K. According to this picture, our measurements, taken at room temperature, were done on the disordered phase of the system. The existence of a long-range charge order is not considered in our model calculations, where we assume that the octahedral site ions have well-defined valence (either +2 or +3) regardless of the electron hopping between Fe^{2+} and Fe^{3+}. The total spectrum is then obtained by summing the contributions from the three Fe sites reported in Figs. 3(b)–3(d). All calculated spectra are expressed as the imaginary part of the optical index, i.e., on a dimensionless absolute scale, and the experimental curve has been multiplied by an arbitrary scaling factor. The chemical shifts between the three contributions have been chosen to fit the experimental absorption of Fig. 3(a) and the magnetic circular dichroism in the resonant reflectivity of Fig. 4(a). We have found the best agreement when the L_3 peak of $Fe^{3+}_{T_d}$ lies 1.05 eV above the $Fe^{2+}_{O_h}$ L_3 peak and 0.6 eV below the $Fe^{3+}_{O_h}$ one. These chemical shifts are very close to those found by Kuiper *et al.*[2]

The Slater integral reductions for $2p$-$3d$ and $3d$-$3d$ interactions were taken equal to 80% and 70% respectively, as in Ref. 2. The parameter δ has been fixed to 0.45 eV for the tetrahedral site (equivalent to the value $10Dq = -0.6$ eV chosen by Kuiper *et al.*) and to 0.5 eV for the octahedral site. This latter value corresponds to $10Dq = 1.5$ eV, which is slightly lower than the value 1.6 eV reported in Ref. 2. Our choice of a lower δ for the octahedral sites is necessary to obtain the right magnetic properties of Fe_3O_4, whose tetrahedral sites are spin up and whose octahedral sites are spin down.[14] In fact, for a 70% reduction of $3d$-$3d$ Slater integrals, our calculation gives a high-spin to low-spin transition for the ground state of the Fe^{2+} in octahedral sites between $10Dq = 1.5$ eV and $10Dq = 1.6$ eV, and no magnetic contribution from this site for $10Dq = 1.6$ eV (see Fig. 2). Using $10Dq = 1.6$ eV we would get a slightly better agreement, especially for the shape and position of the L_2 peak, but wrong magnetic properties.

Figure 4(a) compares the experimental and calculated magnetic reflectivity for circularly polarized photons incident at 3° grazing angle on the (111) surface, with the scattering plane perpendicular to $[0\bar{1}1]$ and magnetic field oriented as $\pm[\bar{2}11]$. The magnetic signal is expressed as an asymmetry ratio, i.e., the difference between spectra obtained for opposite magnetization directions divided by their sum. The reflectivity calculation has been done by Kramers-Kronig-transforming the calculated absorption to obtain the dielectric tensor and then by solving Maxwell's equations.[15] The shoulder at energies lower than 705 eV is dominated by the real part of the index. This shoulder is smooth because the $2p$-to-$3d$ transition has no oscillator strength in this region. The sharp peaks around 707 eV are the effect of the strong variation of the dichroism spectrum at these energies [see Fig. 4(b)]. The strong asymmetry around 720 eV is due to the reflectivity minimum located before the L_2 peak.

Although the calculation parameters have been chosen to

fit the asymmetry curve of Fig. 4(a) and the linear polarization absorption spectra of Fig. 3(a), the calculated magnetic circular dichroism (MCD) spectrum of Fig. 4(b) is quite similar to the results by Kuiper *et al.*, obtained by directly fitting the MCD spectrum. The agreement with experiment in Figs. 3(a) and 4(a) is quite satisfactory and comparable to the results reported in previous studies using other ligand-field calculational methods.

V. CONCLUSIONS

We have presented the results of a calculational method that we have developed for the analysis of ligand-field atomic multiplets, with applications in the field of spectroscopic studies of localized electron systems.[8] Our method, based on the same physical assumptions adopted in previous works by other authors,[3–6] considers all the interactions at once, without any additional assumption regarding the hierarchy of perturbation terms, and can treat any geometrical arrangement. For these reasons it can be easily applied to any geometry of the local environment, including magnetic ordering, regardless of the specific ligand-field symmetry group. Compared to the methods that apply symmetry conditions and consider a hierarchy between interactions terms, our approach involves the diagonalization of larger matrices and requires additional computing resources, an aspect that can be dealt with on modern computers.

We have tested our method by calculating the $2p \rightarrow 3d$ transitions of Ni^{2+} for the local environment of the NiPc molecule, including linear polarization dependence. We have also determined the Fe $2p$ absorption spectra and the magnetic circular dichroism in the reflectivity from a thin Fe_3O_4 film, a compound where the coexistence of three distinct Fe sites makes the calculation more complex. In both cases, we obtain good agreement with the experimental results, in terms of absorption line shapes and polarization dependence. In the case of Fe_3O_4, we have also compared our results to those of previous calculations by Kuiper *et al.*,[2] obtaining a generally good agreement with only slight discrepancies in the refinement of certain crystal-field parameters.

ACKNOWLEDGMENTS

We want to thank the optical group of LURE (Orsay) for the use of their computational facility, and Eric M. Gullikson and James H. Underwood for the use of beamline 6.3.2 at the ALS (Berkeley).

[1] F. M. F. de Groot, J. Electron Spectrosc. Relat. Phenom. **67**, 529 (1994), and references therein.

[2] P. Kuiper, B. G. Searle, L.-C. Duda, R. M. Wolf, and P. J. van der Zaag, J. Electron Spectrosc. Relat. Phenom. **86**, 107 (1997).

[3] T. Yamaguchi, S. Shibuya, and S. Sugano, J. Phys. C **15**, 2625 (1982).

[4] B. T. Thole, G. van der Laan, and G. A. Sawatzky, Phys. Rev. Lett. **55**, 2086 (1985).

[5] B. T. Thole, G. van der Laan, and P. H. Butler, Chem. Phys. Lett. **149**, 295 (1988).

[6] G. van der Laan and B. T. Thole, Phys. Rev. B **43**, 13 401 (1991).

[7] P. H. Butler, *Point Group Symmetry, Applications, Methods and Tables* (Plenum, New York, 1981).

[8] A. Mirone, URL:http//www.lure.u-psud.fr/LogicScient/AMARCORD/index.html

[9] R. D. Cowan, *The Theory of Atomic Structure and Spectra* (University of California Press, Berkeley, 1981).

[10] E. U. Condon and H. Odabasi, *Atomic Structure* (Cambridge University Press, London, 1980).

[11] G. Dufour, C. Poncey, F. Rochet, H. Roulet, S. Iacobucci, M. Sacchi, F. Yubero, N. Motta, M. N. Piancastelli, A. Sgarlata, and M. De Crescenzi, J. Electron Spectrosc. Relat. Phenom. **76**, 219 (1995).

[12] See, e.g., V. I. Anisimov, I. S. Elfimov, N. Hamada, and K. Terakure, Phys. Rev. B **54**, 4387 (1996); S. K. Park, T. Ishikawa, and Y. Tokura *ibid.* **58**, 3717 (1998).

[13] M. Sacchi, C. F. Hague, S. Gota, E. Guiot, M. Gautier-Soyer, L. Pasquali, S. Mrowka, E. M. Gullikson, and J. H. Underwood, J. Electron Spectrosc. Relat. Phenom. **101-103**, 407 (1999).

[14] R. A. Lefever, in *Magnetic and Other Properties of Oxides and Related Compounds*, edited by K.-H. Hellwege and A.M. Hellwege, Landolt-Börnstein, New Series, Group III, Vol. 12, Pt. b (Springer-Verlag, Berlin, 1980), p. 55.

[15] M. Sacchi and A. Mirone, Phys. Rev. B **57**, 8408 (1998).